JME
Journal of Mechatronics Engineering

The Use of a Statistical Filter and Metaheuristics to Model and Control the DC Motor of the Mobile Robot Used on NXP Cup

ARTUR FERREIRA MOREIRA[1], ANDRESSA DA SILVA FERNANDES[2], JOSÉ AILTON BATISTA DA SILVA[1], ALAN VINICIUS DE ARAÚJO BATISTA[1], PEDRO HENRIQUE ALMEIDA MIRANDA[1]

[1]Intituto Federal de Educação, Ciência e Tecnologia do Ceará (IFCE), Brazil
[2]Universidade Federal do Ceará (UFC), Brazil

<artur31415926@gmail.com>, <andressafernandes06.af@gmail.com>, <ailton.ifce@gmail.com>, <alan.ifce@gmail.com>, <pedromiranda@ifce.edu.br>

DOI: 10.21439/jme.v1i1.16

Received: 1 Mar. 2018. **Accepted:** 9 Apr. 2018

Abstract. Over the past decades, Robotics is one of the research fields with more advances. From methodologies of low-level control, used on actuators, to high-level control, used with artificial intelligence approaches. One of the most interesting problem that a mobile robot faces is autonomous navigation. For the robot be able to navigate on the environment autonomously, it have to make use of sensory input from one or more sensors that are used to perceive the robot surroundings as well as sensors that measure internal states of the robot. One of the most used control theory methodology is the proportional-integrative-derivative (PID) controller, where its parameters are estimated through a variety of ways, from raw mathematical modeling to the application of hybrid approaches that uses both a mathematical model and metaheuristics such as genetic algorithms. This paper aims to estimate the parameters of the direct current motor through a Kalman filter and use those to estimate the PID parameters to control the DC motor by the usage of a genetic algorithm. Results shows that the derived PID controller is quite efficient on the control of the DC motor used, thus validating the methodology.

Keywords: Direct Current Motor. Genetic algorithms. Kalman filter. Mobile Robot. PID.

1 Introduction

Robotics in one of the most prolific research fields (WANG et al., 2018). Throughout its main topic, the most fascinating one is autonomous navigation (ÖZASLAN et al., 2017). Several algorithms and methodologies can be used to enable a mobile robot to perform autonomous navigation (CHOU; JUANG, 2018). These mainly are divided on two categories: navigation on a known environment and navigation on an unknown environment (VOLKER, 2013). Beyond that, both categories can be divided even further if the environment is dynamic or not (DAHALAN et al., 2017).

To perform the desired navigation, the mobile robot has to use a series of actuators that perform on any mediums ranging from air to ground (GUO et al., 2017). On the use of these actuators, the robot has to take in account the fact that the interaction between the actuator and the environment is not ideal, so that discrepancies between the value set as the control input and the actual value could be considerable, where value here can be a velocity of a motor for example. When the control is done in this fashion, it said that the control is open-loop, in other words, the control is not aware of the error of control variable (SHIH; LIN, 2017).

When the controller is aware of the error of control variable and minimizes it, then it is said that the controller is closed-loop (ZHANG; TRAN; HUANG, 2018). There is a variety of closed loop controllers, each varying in scope, precision, computation complexity and among other aspects (ZHANG; WEI, 2017). One of such controllers is the Proportional-integrative-derivative controller (PID) (TAKAHASHI, 2018). The PID controller is one of the most versatile controllers, used since the analog computer era with applications from automatic ship steering to some of the control procedures used on the Apollo missions (NAKATANI; SANDS, 2018).

One of the key points of the PID controller are its parameters, or weights. There is one for each block of the controller. Each is used to weight the influence of each part of the controller on the error correction of the control variable (XING et al., 2018). There are several methods to estimate these parameters ranging from the mathematical modelling using control theory alone to artificial intelligence models (DOERR et al., 2017). One of the most used metaheuristics of the artificial intelligence is genetic algorithm (WANG, 2017).

Genetic algorithm consists on the simulation of a population, apply evolutionary operators to it at each iteration and watch the changes on the population so that one of its individuals become a good solution to the problem at hand (AL-JARRAH; AL-JARRAH; ROTH, 2018). At each iteration, all individuals of the population are evaluated by a fitness function, derived to measure how good an individual is as a solution to the studied problem, this could be anything from finding the best word to fit on a sentence to the best geometry to an RF antenna (DU; LI; XU, 2016).

Every individual is an encoded version of the parameters that it represents when applied to the problem (LIANG et al., 2017). This encoding scheme can be performed in a variety of ways where the most common is value encoding. Value encoding consists on each gene of an individual is a value, that could be numeric or a string of characters, so that encoding and the decoding procedure consists on inserting and retrieve values from an array, where this array is the individual (AZMI; MAWENGKANG, 2018).

To simulate the population used on the genetic algorithm an environment-agent model is needed (DURIEZ et al., 2016). Since here the individual is the encoded parameters of the PID that controls the direct current (DC) motor, then the model that correlates the interaction between the agent and the environment is the model of the DC motor. Since the DC motor is an electromechanical device, its mathematical model depends on constants of mechanical and electrical nature (SANKARDOSS; GEETHANJALI, 2017). The estimation of those parameters can be done through a variety of methods that can range from raw mathematical modeling to the implementation of heuristics that in one way or another includes the analysis of experimental data collected while the device is operating on certain conditions (GRIGOROV; ATANASOV, 2017). As the analysis, is quite common to use a statistical filter such as the Kalman filter, also known as the linear quadratic estimation (LIU, 2008).

The Kalman filter is a statistic filter that estimates the state variables of the system with the use of a model of the system and with data of some variables of the system that is used to correlate the input that is given to the system with its output (DZIUBEK et al., 2012). This filter is often used to estimate variables such as the position of a robot with respect to the global frame of reference using inertial and rotational sensors with a very small error of estimation (GREENBERG; TAN, 2017). The Kalman filter is also often used to estimate constants of a system that is operating on predefined conditions and the input is known beforehand. In this case, which the processing of the data is done after the experiment, where the first case the filter is implemented while the system is operating, the variables, or constants, are estimated when the data is then gathered (SUN et al., 2017).

With the objective of integrating graduation students on real world engineering problems on a controlled environment some competitions were idealized and put in practice by various entities from universities to conglomerates from a couple of markets. One of such is the NXP Semiconductors that promote, among others, the NXP Cup. This competition have nationals on more than 9 countries with an international phase, since 2012 the competition have a great impact on more than 500 schools and 15,000 students a year (NXP, 2018a).

The NXP Cup promotes various problems on the fields of robotics, signal processing, embedded systems, mechanical engineering, electrical engineering, control engineering, among others to groups of students from around the world. The main task of the competition is to design, build and program a mobile robot that uses Ackerman steering and have as the main sensor one or more cameras. To win the competition the mobile robot of the group has to finish a track with the smallest time possible. This track is built using the standards defined on the competition rules (NXP, 2018b).

The previously cited problems and the standard nature of the competition turns it on an excellent benchmark to research on the field of robotics, in special the field of autonomous navigation in mobile robotics. For that, the competition can be used to implement, improve and develop even further the methodologies of the state of the art of autonomous navigation, even with hybrid implementations such as those who borrow algorithms from the field of artificial intelligence.

With this in mind, this paper aims to model and control the DC motor used on the mobile robot of the NXP Cup with the use of a Kalman filter to estimate the DC Motor parameters and a genetic algorithm to estimate the parameters used on the PID controller.

2 Methodology or Materials and Methods

implement the PID controller, the model of the main actuator and of the sensors and actuators used needs to be derived so that these can be used to estimate the control parameters. The principal sensor used is an odometry sensor, here and optical encoder, and the actuator is a DC motor.

2.1 Direct Current Motor

The DC Motor can be modelled as a electromechanical device, where a continuous electrical current produces an electromagnetic field on the coils and through interaction with the magnetic field of the permanent magnets on the motor chassis, a torque is generated on the same axis that the coils are attached (BALAMURUGA; MAHALAKSHMI, 2017). From (GLOWACZ; GLOWACZ, 2007) we have:

$$\frac{di_a(t)}{dt} = \frac{(V_a(t) - R_a(t) \cdot i_a(t) - k_\omega \omega(t)}{L_a} \tag{1}$$

$$\frac{d\omega(t)}{dt} = \frac{(k_T \cdot i_a(t) - B\omega(t) - T_l(t)}{J} \tag{2}$$

Where $i_a(t)$ is the armature current, $V_a(t)$ is the armature voltage, $R_a(t)$ is the armature resistance, $\omega(t)$ is the angular velocity of the shaft, L_a is the motor inductance, k_ω is a voltage coefficient, B is the friction coefficient , J is the inertia moment of the load. $V_a(t)$ on the previous equation can be substituted by $V_{pwm}(t) \cdot k_{pwm}$, where $V_{pwm}(t)$ is the PWM used to control the motors speed and k_{pwm} is the constant that relates the PWM to the output voltage of the controller. Then the equation becomes:

$$\frac{di_a(t)}{dt} = \frac{V_{pwm}(t) \cdot k_{pwm} - R_a(t) \cdot i_a(t) - k_\omega \omega(t)}{La} \tag{3}$$

2.2 Encoder of Revolution

To estimate the travelled distance of each wheel, theirs angular displacement must be estimated and for that, the most common sensors are the Hall Effect and the revolution encoder sensors. The revolution encoder consists on an electromechanically device that converts an angular position or the angular velocity of the axis on a signal that can be either analog or digital (ALBRECHT et al., 2017).

There are two types of encoders, absolute and relative, where the first can determine at each time the absolute angular position of the axis and the second can only determine how much the angle has changed, without any indication of the initial angular position on the shaft (PARK et al., 2017).

The errors on the estimative of the angular position using encoders are cumulative by nature, what makes the encoders with low resolution with little to no use on situations that the robot has to operate on a long period. Furthermore, encoders are the best devices to infer the angular displacement on systems that have angular motion (TOLEDO et al., 2018).

2.3 Odometry

Odometry by itself has several factors that can diminish the precision of the pose estimation, one of such is the fact that the wheels of the mobile robot can slip, and such error source as well as others from an odometry implementation are cumulative. The imprecision of the values used on the system constants like the diameter of the wheels can have a big impact on the odometry system (BORENSTEIN; FENG, 1996).

Calling j as the index of the side of the wheel, where $j = I$ is the internal and $j = E$ is the external, and considering that both encoders have the same number of pulses per revolution N_{PRev} and that N_{WI} and N_{WE} are the measured pulses by the encoder on the internal and external wheel, respectively, on the kth iteration, the angle of the internal wheel η_{WI} and of the external wheel η_{WE} on the kth iteration can be both calculated by:

$$\eta_{\omega j_k} = 2\pi G_{R_\omega} \left(\frac{N_{\omega j_k}}{N_{PRev}} \right) \tag{4}$$

Where G_{R_ω} is the transmission relation between the encoder axis and the wheel axis. From the previous equation, the angular speed of the jth wheel (ωj_k) can be obtained by:

$$\omega j_k = \frac{\eta_{\omega j_k} - \eta_{\omega j_{k-1}}}{T_s} = \frac{2\pi G_{R_\omega}}{T_s} = \left(\frac{N_{\omega j_k} - N_{\omega j_{k-1}}}{N_{PRev}}\right) \quad (5)$$

To know the angular speed of the jth attached motor to the jth wheel, all that is needed is to multiply the transmission relation between the encoder and the motor G_{R_M} and G_{R_ω}.

$$\omega_{Mj_k} = \omega_{Wj_k}\left(\frac{G_{R_M}}{G_{R_\omega}}\right) \quad (6)$$

The travelled distance by the jth wheel is estimated using equation 3 and the wheel's radius R_w.

$$\Delta S_{\omega j_k} = S_{\omega j_k} - S_{\omega j_{k-1}} = R_\omega \eta_{\omega j_k} \quad (7)$$

2.4 Direct Current Motor Speed Control

The difference between the desired velocity, or set point, of the jth wheel $\omega^S_{Wj_k}$ and the kth estimated speed of the jth wheel ω_{Wj_k} is:

$$e_{wjk} = \omega^S_{Wj_k} - \omega_{Wj_k} \quad (8)$$

The value of e_{wjk} is used as the error on a discrete PID algorithm. On the discretization procedure of the general equation of the PID controller, the derivative part is simplified using the right rectangular rule and the integrative part is simplified using the Tustin transformation (GOHARI, 2006). The discrete version of the general equation of the PID can be seen down below.

$$\frac{de_j(t)}{dt} \cong \delta_{wjk} = \frac{e_{wj_k} - e_{wj_{k-1}}}{T_s} \quad (9)$$

$$\begin{gathered}\int_0^{kT_s} e_{wj}(t)dt = \\ \int_0^{kT_s-T_s} e_{wj}(t)dt + \int_{kT_s-T_s}^{kT_s} e_{wj}(t)dt \\ \Rightarrow \int_0^{kT_s} e_{wj}(t)dt \cong \sigma_{wjk} = \\ \sigma_{wjk-1} + \frac{e_{wjk} + e_{wjk-1}}{2}T_s \end{gathered} \quad (10)$$

Calling u_{wjk} as the kth control variable of the jth wheel we have:

$$u_{wjk} = K_p e_{wjk} + K_p \sigma_{wjk} + K_p \delta_{wjk} \quad (11)$$

Where K_p, K_i and K_d are the PID parameters used to control the motors. Here K_p, K_i and K_d are assumed to be the same of both motors, what does not happens in practice, but since both motors are the same model from the same manufacturer, the difference of those parameters between both motors are so small that here it is considered negligible.

Both motors are controlled by a Pulse-Width Modulation (PWM) of 8 bits, so u_{wjk} needs to be restricted on the interval of $[0, u_{MAX}]$, where $0 < u_{MAX} \leq 255$. u_{MAX} is smaller than 255 so that the DC motor doesn't get damaged while operating.

2.5 Estimation of the DC motor parameters using a Kalman Filter

Here are a variety of methods that can be used to estimate the constants used on the mathematical model of the DC motor. The most common ones make use of analysis of experimental data collected of the motor while it operates on certain conditions. As the analysis, is quite common to use a statistical filter such as the Kalman filter, also known as the linear quadratic estimation (LIU, 2008).

Kalman filter equations used come from (KHAN et al., 2017). The Kalman filter will have as output a matrix with all the constants of the DC motor.

$$\Lambda^M = [R_a\ L_a\ k_\omega\ k_t\ B\ J\ k_{pwm}] \quad (12)$$

To collect the data used on the filter a constant voltage is applied to the DC motor and the instantaneous values of the armature current i_a and shaft angular velocity ω are measured with the motor without load.

2.6 Estimation of the PID Parameters Using Genetic Algorithms

With the values from the DC motor constants the only thing left is to derive the values for K_p, K_i and K_d for the PID of the motors. This estimation can be performed by several methods. Between those methods are the least squares method and its variants, gradient descent, some machine learning algorithms, among others (ELSROGY; FKIRIN; HASSAN, 2013). Between these methods is genetic algorithms (GA), also known as genetic computing.

A is a metaheuristic that simulates the process of natural selection on individuals of a population through genetic operators such as mutation and crossover in silico. GA is mostly used to solve problems that requires the fine-tuning of a certain number of parameters with a low computing cost and a high probability of reaching the global minima (YANG, 2017).

Defining Y_{l_j} as the jth individual of the lth population, then this individual is an optimal solution if its fitness $\phi(Y_{lj})$ has the smallest value of the lth population when $l = l_{MAX}$ or if $\phi(Y_{lj}) < \phi_d$, where ϕ_d is the desired fitness and l_{MAX} is the maximum number of allowed iterations to the genetic algorithm.

The fitness function is responsible to evaluate every individual and to assign a value to it that corresponds to its performance as the solution of the problem, where the problem is the values of the parameters K_p, K_i and K_d for the PID controller. The function $\phi(Y_{lj})$ is then proposed to model the behavior of the general way that a PID controller modifies the output signal. This can be seen on Figure 1.

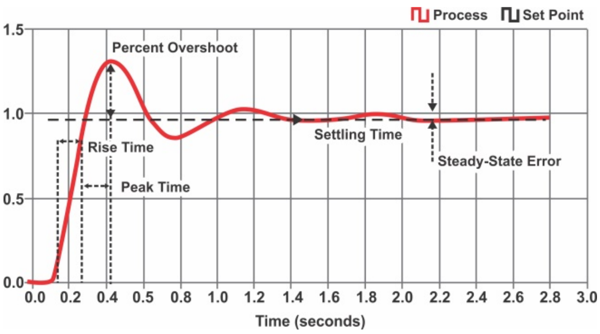

Figure 1: Main characteristics of the PID controller. Source: The Authors, 2018.

Considering O_v as the overshoot, τ_r as the rising time, τ_s as the stabilization time, τ_p peak time and ε_s steady-state error, the fitness function is then modeled as:

$$\phi(Y_{lj}) = \alpha_{o_v} O_v + \alpha_{\tau_r}\tau_r + \alpha_{\tau_s}\tau_s + \alpha_{\tau_p}\tau_p + \alpha_{\varepsilon_s}\varepsilon_s \quad (13)$$

Where α_{o_v}, α_{τ_r}, α_{τ_s}, α_{τ_p} and α_{ε_s} are weighting constants and theirs values are determined empirically. The GA implemented here uses the elite operator, where at each population the best are selected as the elite individuals and are used to breed with the other members of the population, but never with themselves. The value of N_E is often set to a small value and it is expressed in a proportional way to the number of individuals of the population N_p, where the proportional constant is v_E. N_E is shown on 14:

$$N_E = v_E N_p \quad (14)$$

The crossover operator ψ is responsible to produce the next generation from the breeding between the members of the elite and the rest of the population, where these are selected for breeding using the pool selection algorithm. ψ uses a single delimiter on the genes of the parent individuals and generates two individuals as children.

Of all the ways that the mutation operator μ can affect the genes of the individuals (LIM et al., 2017), here the mutation is performed by adding a random value from the interval of $[-\gamma, \gamma]$ to a random selected index i_μ. Where γ is chosen to be a value closer to zero and $0 \leq i_\mu \leq N_G^P$ and N_G^P is the number of genes of the individual. μ is only applied to an individual if a random value from the interval $[0, 1]$ is smaller than the mutation rate μ, where this rate is preferred to be kept small when a more stable and reliable solution is desired.

Here also the immigration wave operator is used (HONG et al., 2017). Where this operator is responsible to simulate an immigration of a number of individuals N_I with random initialized genes to the next population. Immigration creates a wide search space so that the chance of all individuals on a certain population to be stuck on a local minima is very unlikely. The value of N_I is chosen to be a value that is proportional to N_P, where the constant of proportionality is v_I.

$$N_I = v_I N_P \quad (15)$$

On the initialization, the first population have all of its individuals initialized with random genes on the interval of $[-\lambda, \lambda]$, where λ is usually keep close to 1.

3 Results and discussion

3.1 Estimation of the DC motor parameters

During the experimental trials, an oscilloscope with direct connection with Matlab were implemented. The measured parameters were the RMS (Root Mean Square) of the motor current and the period of the waveform of the encoder that is attached on the motor axis by two gears. Those can be seen on Figures 2 and 3. From the kth period measured T_{Pk}, the kth angular velocity ω_k^E is then estimated by the following equation.

$$\omega_k^E = G_{R_M}\left(\frac{2\pi}{P_{rev}}\right)\frac{1}{T_{Pk}}(rad/s) \quad (16)$$

Where the transition relation between the encoder and the motor is $G_{R_M} = 43/9$ and the encoder have $P_{rev} = 500$ pulses per revolution. Beyond that, the raw

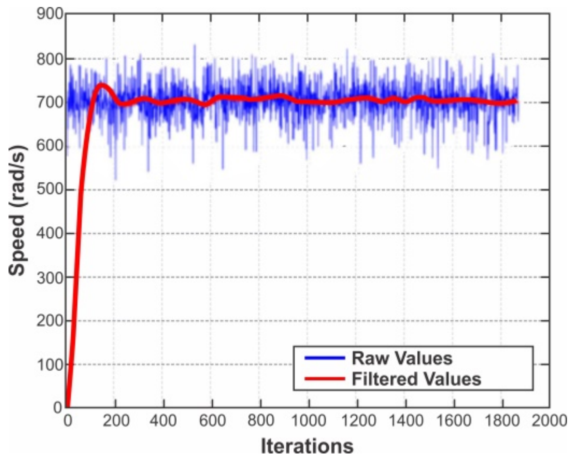

Figure 2: Waveform on the estimated angular velocity of the DC motor and its filtered waveform. Source: The Authors, 2018.

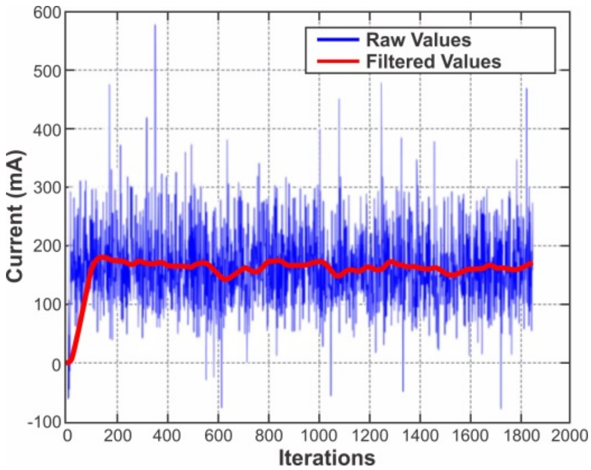

Figure 3: Waveform of the current signal of the DC motor and its filtered waveform. Source: The Authors, 2018.

data is then filtered by the means of a low-pass filter, the butterworth filter (DWIVEDI; BHATT; GHOSH, 2017).

During the trials, the motor was receiving a voltage of 3 V and for simplicity sake, the ideal value of the voltage will be used on the Kalman filter algorithm. The constants used on the filter have the following values:

$$\gamma = 0.93; \psi = 0.07; \varepsilon_D = 10^{-4} \tag{17}$$

By the use of the Kalman filter and the processed data and Defining V_{BAT} as the voltage of the battery and dividing it by 2^8, since the controller used have 8 bits, then Λ^M have the values of 18.

$$\Lambda^M = \begin{bmatrix} R_a = 2.7598542435 87(\Omega) \\ L_a = 1.1186575703 \times 10^{-2}(H) \\ k_\omega = 5.008705 \times 10^{-3}(V/(rad/s)) \\ k_T = 5.008705 \times 10^{-3}(Nm/A) \\ B = 1.13284 \times 10^{-6}(Nm/(rad/s)) \\ J = 2.2748 \times 10^{-8}(Nm/(rad/s^2)) \\ k_{pwm} = \frac{V_{BAT}}{255}(V) \end{bmatrix} \tag{18}$$

For the comparison with the model of the motor using Λ^M and the physical device, the model was simulated applying the ideal voltage of 3 V and the results of the simulation are shown together with the collected data of the physical device. Those can be seen on Figures 4 and 5.

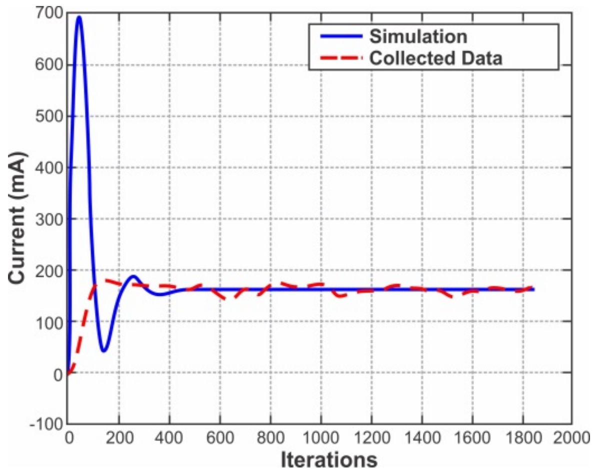

Figure 4: Comparison between the current of the simulation of the DC motor and the data that was gathered previously. Source: The Authors, 2018

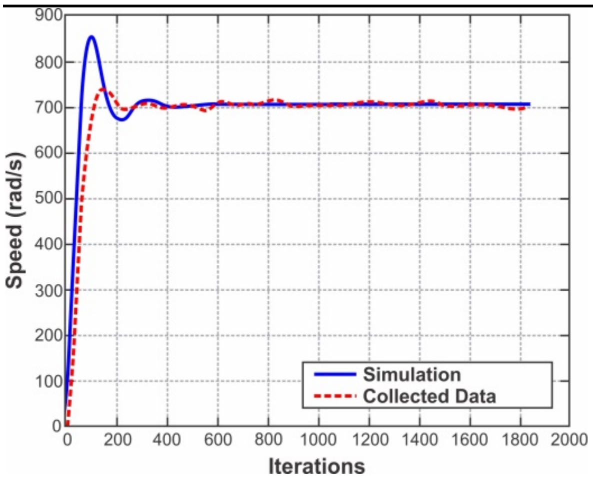

Figure 5: Comparison between the angular speed of the simulation of the DC motor and the data that was gathered previously. Source: The Authors, 2018.

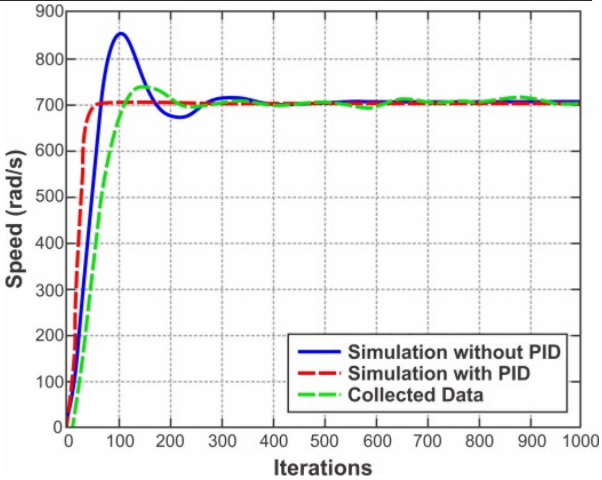

Figure 6: Comparison between the simulation of the DC motor with and without the estimated PID parameters and the collected data. Source: The Authors, 2018.

3.2 Estimation of the PID parameters of the DC motor controller

The constants used on the genetic algorithm were deliberately chosen to be as follows.

$$k_{MAX} = 600; \phi_D = 10^{-4}; N_P = 500; \\ v_E = 10; v_I = 10; \mu_R = 0.2; \quad (19)$$

After 3 hours, the algorithm completed iterations with the individual with the smallest fitness with the value of 0.042438. Converting the values of this individual to the values of the PID parameters we have that $K_P = 19.102365736574$, $K_i = 0.000859285929$ and $K_d = 0.025063706371$.

As comparison, the DC motor was simulated with and without the PID using the values of the parameters estimated previously and the data collected previously is compared to the simulation. All this can be seen on Figure 6.

The values of O_v, τ_R, τ_P, ϵ_R and τ_s of the three cases shown on Figure 6 are shown on Figure 7.

4 Conclusion

On the present work the modeling of the DC motor is derived through the estimative of the motor parameters by the use of a Kalman filter and data collected on the real derive working without load and the parameters of a PID controller are then estimated by the use of a genetic algorithm. The data obtained of the simulated experiments of both the DC motor mathematical model as well as its control by the PID controller shows that the proposed methodology satisfies its objectives. That is evident on the values of overshoot, rising time, stabilization time, peak time and steady-state error of the angular velocity of the simulated DC motor controlled by the derived PID. The values of those variables when the PID is used are significantly smaller when compared with the values of the simulation of the DC motor without the use of a PID controller and even more when compared with the data collected of the real device operating on a continues voltage.

On a future work, a more advanced hardware for simulation will be used to test the proposed methodology on other interesting cases such as navigation in and out of a t shaped intersection, as well as many others. The hardware implementation on an actual mobile robot will be studied and its results will be used as a validation mechanism to the current methodology, since the simulated environment is used as a benchmark to speed up research and development of the methodology proposed on this paper.

References

AL-JARRAH, R.; AL-JARRAH, M.; ROTH, H. A novel edge detection algorithm for mobile robot path planning. **Journal of Robotics**, Hindawi, v. 2018, 2018.

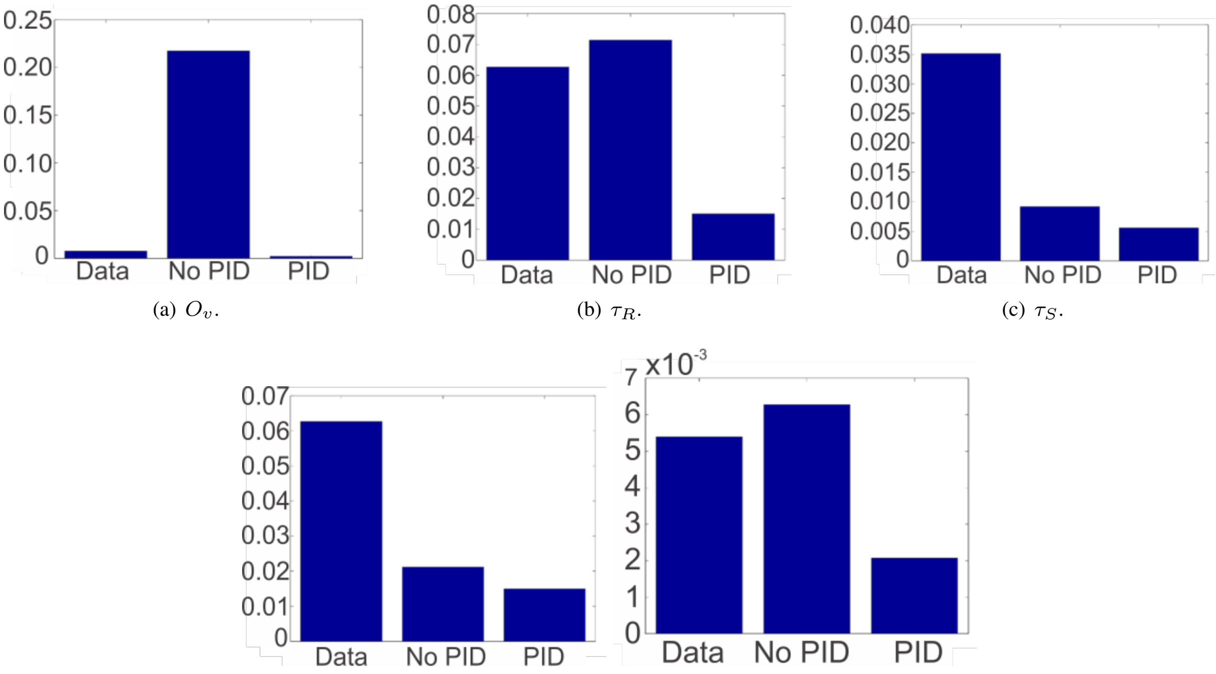

(a) O_v. (b) τ_R. (c) τ_S.

(d) τ_P. (e) ϵ_S.

Figure 7: O_v, τ_R, τ_S, τ_P and ϵ_S for the comparison between simulation and the collected data. Source: The Authors, 2018.

ALBRECHT, C.; KLÖCK, J.; MARTENS, O.; SCHUMACHER, W. Online estimation and correction of systematic encoder line errors. **Machines**, Multidisciplinary Digital Publishing Institute, v. 5, n. 1, p. 1, 2017.

AZMI, Z.; MAWENGKANG, H. Perceptron genetic to recognize openning strategy ruy lopez. In: IOP PUBLISHING. **IOP Conference Series: Materials Science and Engineering**. [S.l.], 2018. v. 300, n. 1, p. 012069.

BALAMURUGA, K.; MAHALAKSHMI, R. Parameter identification in bldc motor using optimization technique. **Journal of Applied Science and Engineering Methodologies**, Journal of Applied Science and Engineering Methodologies, v. 3, n. 2, p. 465–470, 2017.

BORENSTEIN, J.; FENG, L. Measurement and correction of systematic odometry errors in mobile robots. **IEEE Transactions on robotics and automation**, IEEE, v. 12, n. 6, p. 869–880, 1996.

CHOU, C.-Y.; JUANG, C.-F. Navigation of an autonomous wheeled robot in unknown environments based on evolutionary fuzzy control. **Inventions**, Multidisciplinary Digital Publishing Institute, v. 3, n. 1, p. 3, 2018.

DAHALAN, A.; SAUDI, A.; SULAIMAN, J.; DIN, W. Numerical evaluation of mobile robot navigation in static indoor environment via egaor iteration. In: IOP PUBLISHING. **Journal of Physics: Conference Series**. [S.l.], 2017. v. 890, n. 1, p. 012064.

DOERR, A.; NGUYEN-TUONG, D.; MARCO, A.; SCHAAL, S.; TRIMPE, S. Model-based policy search for automatic tuning of multivariate pid controllers. In: IEEE. **Robotics and Automation (ICRA), 2017 IEEE International Conference on**. [S.l.], 2017. p. 5295–5301.

DU, L.; LI, L.; XU, Y. A genetic antenna selection algorithm with heuristic beamforming for massive mimo systems. In: IEEE. **Wireless Personal Multimedia Communications (WPMC), 2016 19th International Symposium on**. [S.l.], 2016. p. 49–52.

DURIEZ, C.; COEVOET, E.; LARGILLIERE, F.; MORALES-BIEZE, T.; ZHANG, Z.; SANZ-LOPEZ, M.; CARREZ, B.; MARCHAL, D.; GOURY, O.;

DEQUIDT, J. Framework for online simulation of soft robots with optimization-based inverse model. In: IEEE. **Simulation, Modeling, and Programming for Autonomous Robots (SIMPAR), IEEE International Conference on**. [S.l.], 2016. p. 111–118.

DWIVEDI, A. K.; BHATT, S. K.; GHOSH, S. Fractional order butterworth filter design using artificial bee colony algorithm. In: IEEE. **Embedded Computing and System Design (ISED), 2017 7th International Symposium on**. [S.l.], 2017. p. 1–5.

DZIUBEK, N.; WINNER, H.; BECKER, M.; LEINEN, S. Sensordatenfusion zur hochgenauen ortung von kraftfahrzeugen mit integrierter genauigkeits-und integritätsbewertung. In: **5. Tagung Fahrerassistenz**. [S.l.: s.n.], 2012.

ELSROGY, W. M.; FKIRIN, M.; HASSAN, M. M. Speed control of dc motor using pid controller based on artificial intelligence techniques. In: IEEE. **Control, Decision and Information Technologies (CoDIT), 2013 International Conference on**. [S.l.], 2013. p. 196–201.

GLOWACZ, Z.; GLOWACZ, W. Mathematical model of dc motor for analysis of commutation processes. In: IEEE. **Diagnostics for Electric Machines, Power Electronics and Drives, 2007. SDEMPED 2007. IEEE International Symposium on**. [S.l.], 2007. p. 138–141.

GOHARI, P. Lecture 6: Discrete equivalents. **Course: ELEC**, v. 6061, 2006.

GREENBERG, J. N.; TAN, X. Kalman filtering-aided optical localization of mobile robots: System design and experimental validation. In: AMERICAN SOCIETY OF MECHANICAL ENGINEERS. **ASME 2017 Dynamic Systems and Control Conference**. [S.l.], 2017. p. V002T21A013–V002T21A013.

GRIGOROV, I. V.; ATANASOV, N. R. Application of recursive methods for parameter estimation in adaptive pole placement control of dc motor. In: IEEE. **Electrical Machines, Drives and Power Systems (ELMA), 2017 15th International Conference on**. [S.l.], 2017. p. 215–218.

GUO, P.; KIM, H.; VIRANI, N.; XU, J.; ZHU, M.; LIU, P. Exploiting physical dynamics to detect actuator and sensor attacks in mobile robots. **arXiv preprint arXiv:1708.01834**, 2017.

KHAN, A. U. R.; MEHDI, H.; SALEEM, S. M. A.; RABBANI, M. J. A comparison of predictive parameter estimation using kalman filter and analysis of variance. **INTERNATIONAL JOURNAL OF ADVANCED COMPUTER SCIENCE AND APPLICATIONS**, SCIENCE & INFORMATION SAI ORGANIZATION LTD 19 BOLLING RD, BRADFORD, WEST YORKSHIRE, 00000, ENGLAND, v. 8, n. 8, p. 441–446, 2017.

LIANG, Y.; HONG, F.; LIN, Q.; BI, S.; FENG, L. Optimization of robot path planning parameters based on genetic algorithm. In: IEEE. **Real-time Computing and Robotics (RCAR), 2017 IEEE International Conference on**. [S.l.], 2017. p. 529–534.

LIM, S. M.; SULTAN, A. B. M.; SULAIMAN, M. N.; MUSTAPHA, A.; LEONG, K. Crossover and mutation operators of genetic algorithms. **INTERNATIONAL JOURNAL OF ADVANCED COMPUTER SCIENCE AND APPLICATIONS**, v. 7, n. 1, p. 9–12, 2017.

LIU, Z. **Design and Simulation of a LQG Optimal Controller for a Mobile Cart**. [S.l.]: Department of Electrical & Computer Engineering, Temple University, 2008.

NAKATANI, S.; SANDS, T. Battle-damage tolerant automatic controls. **Electrical and Electronic Engineering**, Scientific & Academic Publishing, v. 8, n. 1, p. 10–23, 2018.

NXP. **NXP Cup Overview**. 2018. Disponível em: <https://community.nxp.com/docs/DOC-1011>. Acesso em: 01 jan. 2018.

____. **The NXP Cup Rules 2017-2018 EMEA Rules**. 2018. Disponível em: <https://community.nxp.com/servlet/JiveServlet/download/335083-3-411052/NXP%20Cup%202017_18%20EMEA%20Rules_NEW.pdf>. Acesso em: 01 jan. 2018.

ÖZASLAN, T.; LOIANNO, G.; KELLER, J.; TAYLOR, C. J.; KUMAR, V.; WOZENCRAFT, J. M.; HOOD, T. Autonomous navigation and mapping for inspection of penstocks and tunnels with mavs. **IEEE Robotics and Automation Letters**, IEEE, v. 2, n. 3, p. 1740–1747, 2017.

PARK, J. W.; NGUYEN, H. X.; TRAN, T. N.-C.; JEON, J. W. Improve efficiency multi-turn magnetic encoder that uses gear system. In: IEEE. **Control, Automation and Systems (ICCAS), 2017 17th International Conference on**. [S.l.], 2017. p. 318–324.

SANKARDOSS, V.; GEETHANJALI, P. Parameter estimation and speed control of a pmdc motor used in wheelchair. **Energy Procedia**, Elsevier, v. 117, p. 345–352, 2017.

SHIH, C.-L.; LIN, L.-C. Trajectory planning and tracking control of a differential-drive mobile robot in a picture drawing application. **Robotics**, Multidisciplinary Digital Publishing Institute, v. 6, n. 3, p. 17, 2017.

SUN, Q.; DIAO, M.; ZHANG, Y.; LI, Y. Cooperative localization algorithm for multiple mobile robot system in indoor environment based on variance component estimation. **Symmetry**, Multidisciplinary Digital Publishing Institute, v. 9, n. 6, p. 94, 2017.

TAKAHASHI, M. Self-repairing adaptive pid control for plants with sensor failures. In: **International Conference on Artificial Life and Robotics - ICAROB**. [S.l.: s.n.], 2018.

TOLEDO, J.; PIÑEIRO, J. D.; ARNAY, R.; ACOSTA, D.; ACOSTA, L. Improving odometric accuracy for an autonomous electric cart. **Sensors**, Multidisciplinary Digital Publishing Institute, v. 18, n. 1, p. 200, 2018.

VOLKER, W. Maschinelles sehen für mobile roboter: Virtuell-aktive visuelle odometrie. **at-Automatisierungstechnik Methoden und Anwendungen der Steuerungs-, Regelungs-und Informationstechnik**, Oldenbourg Wissenschaftsverlag GmbH, v. 61, n. 4, p. 269–277, 2013.

WANG, C.; LIU, X.; YANG, X.; HU, F.; JIANG, A.; YANG, C. Trajectory tracking of an omni-directional wheeled mobile robot using a model predictive control strategy. **Applied Sciences**, Multidisciplinary Digital Publishing Institute, v. 8, n. 2, p. 231, 2018.

WANG, J. 34. intelligent control model of pid parameter tuning based on criterion function. **Boletín Técnico, ISSN: 0376-723X**, v. 55, n. 9, 2017.

XING, H.; GUO, S.; SHI, L.; HE, Y.; SU, S.; CHEN, Z.; HOU, X. Hybrid locomotion evaluation for a novel amphibious spherical robot. **Applied Sciences**, Multidisciplinary Digital Publishing Institute, v. 8, n. 2, p. 156, 2018.

YANG, G. Game theory-inspired evolutionary algorithm for global optimization. **Algorithms**, Multidisciplinary Digital Publishing Institute, v. 10, n. 4, p. 111, 2017.

ZHANG, D.; WEI, B. On the development of learning control for robotic manipulators. **Robotics**, Multidisciplinary Digital Publishing Institute, v. 6, n. 4, p. 23, 2017.

ZHANG, T.; TRAN, M.; HUANG, H. Design and experimental verification of hip exoskeleton with balance capacities for walking assistance. **IEEE/ASME Transactions on Mechatronics**, IEEE, 2018.